LAB ON A CHIP

Photochemical reactions and on-line UV detection in microfabricated reactors

Hang Lu,[a] Martin A. Schmidt[b] and Klavs F. Jensen*[a]

[a] *Department of Chemical Engineering, Massachusetts Institute of Technology, Cambridge, MA 02139, USA. E-mail: kfjensen@mit.edu; Fax: +1 617 258 8224*
[b] *Microsystems Technology Laboratories, Massachusetts Institute of Technology, Cambridge, MA 02139, USA*

Received 8th May 2001, Accepted 3rd July 2001
First published as an Advance Article on the web 9th August 2001

This work presents an application of microfabricated reactors and detectors for photochemical reactions. Two fabrication schemes were demonstrated for the integration of the reaction and the detection modules: coupling individually packaged chips, and monolithic integration of the two functions. In the latter fabrication scheme, we have succeeded in bonding quartz wafers to patterned silicon wafers at low temperature using a Teflon-like polymer—CYTOP™. Using quartz substrates allows reaction and detection with UV light of lower wavelengths than Pyrex substrates permit. The pinacol formation reaction of benzophenone in isopropanol was the model reaction to demonstrate the performance of the microreactors. The extent of reaction was controlled by varying the flow rate and therefore the on-chip residence time. Crystallization of the product inside the microreactors was avoided by the continuous-flow design. Instead, crystallization was observed in the effluent storage device. Off-chip analysis using HPLC confirms the results obtained from the on-line UV spectroscopy. The quantum yield estimated suggests that the reactor design is effective in improving the overall efficiency of the reactor unit.

1. Introduction

In chemical synthesis, photochemical reactions are usually cleaner and more efficient than other types of reactions because the key reagent is light of particular energy.[1] Aside from photolithography for the microelectronic industries, important applications of photochemistry include photopolymerization, photo-halogenation, nitrosation, sulfochlorination, and oxidation.[2] In fine chemical syntheses and pharmaceutical productions, photochemical reaction steps offer shorter routes for many synthetic schemes, *e.g.* synthesis of vitamin D. In addition, photocleavage has also become one of the more effective methods for removing protective groups.[3] The use of photochemistry, however, is limited by concerns about scalability, efficiency, and safe operations of the processes. We demonstrate here an improvement in the applicability and efficiency of photochemical reactions by using microfabricated reactors.

Large-scale photochemical reactions are usually performed with macro-scale lamps immersed in the reaction vessel. In most cases, it takes considerable effort to transform a successful lab-scale reaction to its industrial counterpart.[1] Issues involved include the scalability of light sources, heat and mass transfer in the processes, and safety concerns (*e.g.* explosions caused by excess heat).[1,2] Many of the photochemical reactions proceed *via* a free-radical mechanism. If the radicals, which are formed near the light sources, do not diffuse quickly to react further with other species, they are likely to recombine, generating excess heat instead of a productive reaction. Radical recombination reduces the quantum efficiency of the overall process.[1] By miniaturization, however, the diffusive transport of these species effectively reduces the concentration near the light source, and increases the probability that they will collide with other molecules to produce the desired products. The energy from the light source is then fully used for reactions. A more important issue that is unique to photochemical reactions is photon absorption. Many reaction mixtures have components (either the solvent or solutes) that strongly absorb the incident light. In large-scale designs of photochemical reactors, the solutions attenuate the light so that irradiation falls off exponentially from the light source. Therefore the efficiency of such reaction units is reduced. Miniaturizing photochemical reactors takes advantage of the high surface-to-volume ratio and the small length scales of microfabricated devices. At the micro-scale, the solution that fills the reactor is only hundreds of microns deep, allowing light to penetrate through most of the reactor depth.

Motivated by these advantages, we have designed and fabricated microreactors for photochemistry using silicon and related microfabrication technologies. In the recent decade, these technologies, which developed from the microelectronics industry, have enabled device miniaturization. Microfabrication not only includes photolithography, thin-film deposition, and chemical etching of silicon substrates, but also microelectromechanical-systems (MEMS)-specific techniques (*e.g.* wafer bonding, and deep reactive ion etching) and materials (*e.g.* glass and polymers). The applications have expanded from MEMS, to chemical, biochemical, and biomedical devices, improving the sensitivity, accuracy, and performance of traditional equipment. For fine chemical synthesis and analysis, these micro-scale devices have faster mass and heat transfer properties, are dominated by surface forces, have high surface-to-volume ratio, and exhibit laminar flow.[4] These properties are attributed to the small length scales of these devices.[4] Performing photochemical reactions at this scale would benefit from these advantages of microfluidic systems.

2. Experimental

In this work, we have fabricated two sets of microchip devices for the purposes of reaction and detection. The major differences between the two sets are outlined in Table 1 for comparison and nomenclature.

 DOI: 10.1039/b104037p

This journal is © The Royal Society of Chemistry 2001

2.1. Device design and fabrication

In the design of the microreactor, we have considered the following requirements for accommodating photochemical reactions: (1) the cover of the device must be transparent to the incident light; (2) the reactor must have a large surface area to receive the maximum amount of light possible; and (3) the device must minimize crystallization and clogging. Two prototype reactors were produced: **device set I** for demonstrating a sequential detection of benzopinacol formation reaction (with incident light of 365 nm in wavelength); and **device set II** for shorter wavelength reactions and immediate on-line detection. The two prototype reactors use different fabrication schemes that are outlined below.

Reactor I was designed to have a serpentine shape to yield a long channel with a large surface area (Fig. 1(A)). The channel was 500 μm in width, and approximately 250 μm deep with vertical sidewalls. This design was realized by timed deep reactive ion etching (DRIE) of a silicon substrate.[5] Wet etching of silicon using KOH is anisotropic, and would have produced undesirable shapes (*e.g.* sharp corners) at the turns of the reaction channel that could induce crystallization. This prototype has a single inlet and a single outlet. Nonetheless, multiple inlets and outlets would not be difficult to produce with the DRIE technology if on-chip mixing of reactants and delamination of product streams become necessary, as in the case of multiphase reaction system.[6] Fig. 1(B) shows the fabrication sequence for this device. A layer of CVD oxide (1.5–2 μm) was first deposited and densified on the Si wafer. A mask with the patterns for the flow channel and inlet/outlet ports was used to pattern a layer of photoresist. We transferred the patterns into the oxide layer using a buffered oxide etch (BOE, ammonium fluoride and hydrogen fluoride in water). The photoresist was then removed in piranha solution (sulfuric acid to hydrogen peroxide, 3 : 1), and then a new layer was coated. A second mask that had only the inlet and outlet was then used to pattern the new layer of photoresist. The resist layer was used to mask the exposed silicon to produce the inlet/outlet patterns (approximately 250 μm) in the first DRIE step. The wafer was then cleaned with piranha solution, exposing the patterned oxide. In the second DRIE step, the oxide layer was the mask for etching the channel and the inlet/outlet, producing through-holes at the inlet/outlet areas and channel that was 250 μm deep. After the residual oxide layer was removed by BOE, the Si wafer was anodically bonded to a Pyrex wafer. Lastly, the bonded wafer was diced to produce individual reactors.

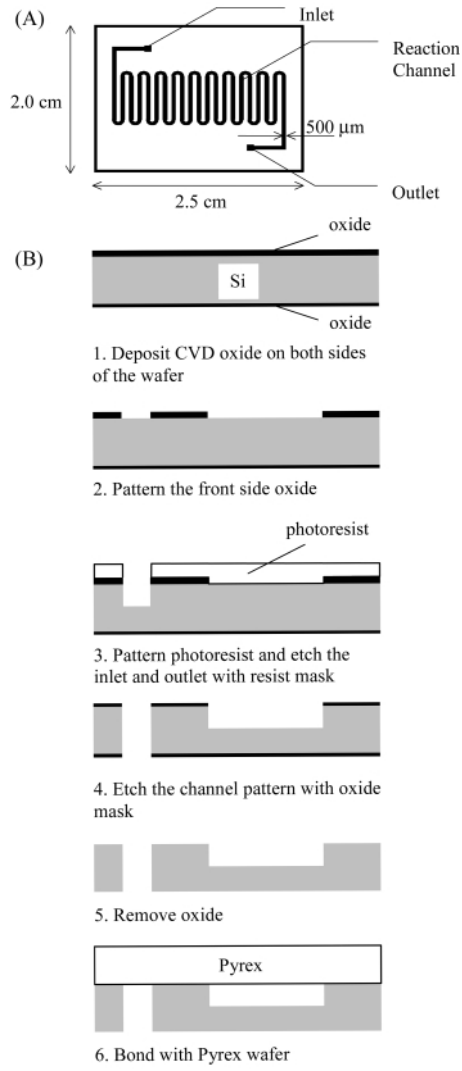

Fig. 1 (A) Design layout of the photochemical-reactor chip I; (B) fabrication sequence of photochemical-reactor chip I—the silicon–Pyrex process.

Detection chip I was fabricated with quartz substrates and a photo-definable epoxy (SU-8) as described by Jackman *et al.*[7] and is transparent to light of wavelengths as short as 200 nm. The device used in the present work is 50 μm deep, and has a straight channel configuration.

The design of reactor chip II was motivated by the integration of the reaction and detection units, and was intended to accommodate reactions that require light of deeper UV (*e.g.* many photochemical reactions require 254 nm light). Pyrex wafers absorb too strongly at these wavelengths to be suitable. To design a detection unit that has an optical path perpendicular to the reactor, part of the reactor has to be transparent from top to bottom. A sandwich structure of a silicon wafer between two quartz wafers was then designed. The top view of the device is shown in Fig. 2(A), and the fabrication sequence is shown in Fig. 2(B). The reaction channel formed in silicon was 500 μm wide, and 500 μm deep (wafer thickness). Corresponding inlet/outlet holes (1 mm in diameter) were drilled in the bottom quartz wafer.

CYTOP™, purchased from Sigma-Aldrich (Milwaukee, WI) as poly(1,1,2,4,4,5,5,6,7,7-decafluoro-3-oxa-1,6-heptadiene), 9 wt.% solution in perfluorotributylamine, was used as a bonding material. The top and bottom quartz wafers were first dehydrated at 90 °C for 20 min on a hot-plate, and cooled to room temperature before spin-coating a thin layer (typically 1–2 μm) of CYTOP™. Then the quartz substrates were heated at 90 °C for 30 min to drive off the solvent in CYTOP™. The bottom quartz wafer with inlet/outlet holes and the silicon wafer were then aligned, and the plain quartz wafer was placed on the top. The wafer stack was then bonded at 160 °C with added weights

Table 1 Micro-photochemical reactor setup and detection devices

Features	Device set I	Device set II
Microchip	Reactor chip I and detection chip I	Reactor chip II
Setup	Macroscopically coupled (2 reactor mounts)	Monolithically integrated (1 reactor mount)
Materials used	Si, Pyrex, SU-8™, quartz	Si, quartz, CYTOP™
Detection	Delayed	Immediate
Typical concentration of benzophenone solution used in the experiments	0.5 M	0.05 M

on top for a minimum of 2 h. The wafer stack was subsequently diced into device chips.

2.2. Reactor assembly scheme and on-line detection setup

Reactor chip I and detection chip I were packaged separately. For the reactor packaging, a machined stainless-steel reactor mount with standard high-pressure fluid fittings was used. A piece of 0.08 cm thick Viton™ (elastomer) material with punched holes served as the gasket that sealed the reactor chip to the steel mount. A clear plexiglass cover plate that was screwed down to the steel mount provided compression seal, sandwiching the reactor and the gasket material. The cover plate also provided housing for the mini UV lamp (BF325-VU1, 365 nm, JKL component, CA) for this reactor. The detection unit was packaged in a similar manner. The mount and cover plate assembly for the detection unit also had an additional pair of through-holes for the integration of optical fibers. Fluid interconnects were standard stainless steel fittings from Up-Church Scientific (Oak Harbor, WA), and 1/16 in PTFE or PEEK tubing was used.

To perform on-line detection, the two mounting units (with the packaged reactor and detection chips) were connected by a 10 cm long HPLC tubing (PEEK). Further, two optical fibers were connected to the detection mount. One of the fibers brought the incident light from a broadband deuterium light source (DT-1000 from Ocean Optics, Inc., Dunedin, FL); the other optical fiber guided the transmitted light to a spectrometer.

The integrated device had a setup that combined the functions of the two mounts described above (Fig. 3). The chip was assembled between a plexiglass plate and a steel mount (with Viton™ gasket) with an opening to house both the optical fibers and the miniature UV lamp. To ensure that the light from the mini UV lamp did not interfere with the detection light, aluminium foil was used to cover the sidewalls of the mini lamp housing. In all experiments, a syringe pump (model PHD2000 from Harvard Apparatus) delivered reaction solutions at specified flow rates.

2.3. Model chemistry testing

In the experiments, benzophenone (> 99.0%) and isopropanol (HPLC grade) purchased from Sigma-Aldrich (St. Louis, MO) were used without further purification. Benzophenone solution in isopropanol (0.5 M) was prepared with the addition of a drop of glacial acetic acid (Sigma-Aldrich).[8] The 0.5 M solution was also diluted with isopropanol to make standards of 0.1 to 0.4 M. The solutions were stored at room temperature without exposure to light for up to two months. Before each run, nitrogen was bubbled through the reactant solution for at least 10 min to deoxygenate the solution.

Before each experiment, the miniaturized UV lamp and the deuterium detection lamp were both turned on for at least 20 min to stabilize light output. The UV lamp was operated with a 5 V DC input (at ~0.20 A) to the inverter, which excites the lamp at 120 V AC. The fluid manifold(s) and the reactor chip(s) were usually flushed with acetone, followed by isopropanol before running an experiment. The entire assembly was then filled with reactant solution. The system was allowed to reach steady state (varying between 1–2 h depending on the flow rate) before spectroscopic data were taken and samples collected. Upon reaching steady state, UV spectra (10 s integration time) of the reaction mixture were obtained in the spectrometer; typically four spectra at different times during a single experiment would be averaged. To calculate the absorbance of a reaction mixture, the transmitted light through pure iso-

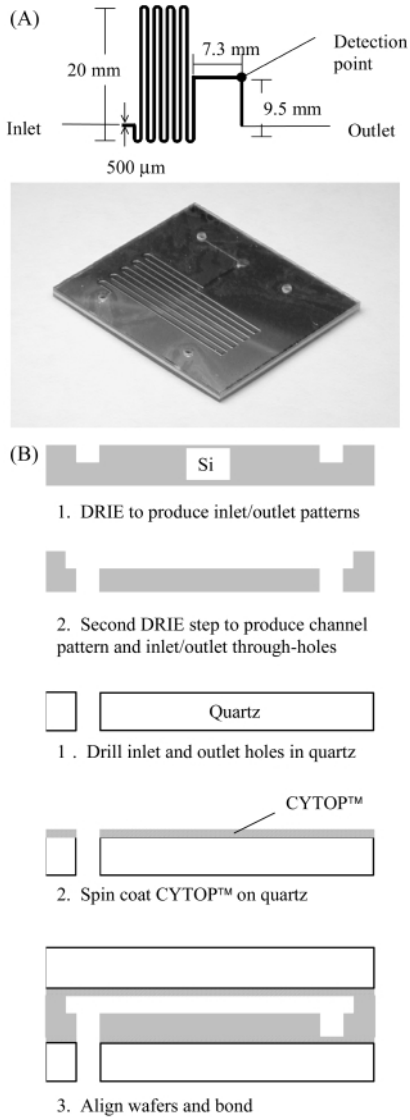

Fig. 2 (A) Design of the integrated reaction–detection unit—reactor chip II; (B) fabrication sequence of reactor chip II—the silicon–quartz process.

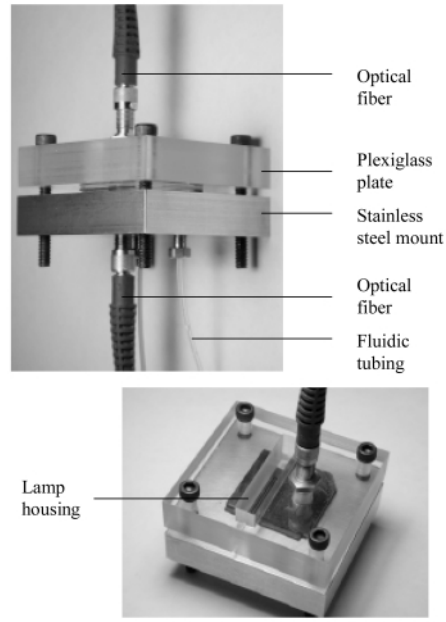

Fig. 3 Photographs of the integrated reactor packaged with chuck, fluid connections, and UV fiber optics.

propanol was used as reference. The same procedure was used to obtain the absorbance of the standard solutions, except with no reaction (achieved by turning off the miniature UV lamp).

Samples were also collected for further analysis with HPLC. A C-18 Econosphere™ column (5 μm packing, 250 × 4.6 mm) from AllTech Associates, Inc. (Deerfield, IL) was used. Typical mobile phase was run at 1 ml min^{-1}, and UV absorbance at 280, 310, 330, and 360 nm were monitored. The analyses were typically performed more than 48 h after collection to ensure complete "dark" reactions (reaction steps following the initial light exposure, but not involving photons). Solutions of benzophenone (0.1–0.4 M) in isopropanol were used to produce standards in UV response in the HPLC. The responses from the reaction samples were then compared to the standard curves to determine the concentrations of species.

The power output of the reaction lamp was measured with a PM3 power probe with PM500D digital power meter, both from Molectron Detector, Inc. (Portland, OR). A silicon chip was etched to have the same pattern as the reactor chips, but all the way through the wafer (500 μm) instead of only halfway through. Together with a piece of a Pyrex wafer, the silicon chip was mounted directly against the PM3 probe detector. The miniature UV lamp was placed on top of the chips in the same manner as for the experimental setup, and voltage was supplied for the normal operation of the lamp. The power meter recorded the power emitted by the mini lamp.

In the monolithically integrated device, since the absorbance path length (500 μm) was 10 times that of the first detection device made in SU-8 (~50 μm), the concentration of the benzophenone solution had to be reduced accordingly to 0.05 M. Our detector was not sensitive enough to detect the transmitted light through a solution of concentration greater than 0.1 M. All other conditions for experiments run in setup II were the same as described above for setup I.

3. Results and discussion

3.1. Fabrication of devices

In fabricating reactor I, we have demonstrated that Pyrex is suitable for photochemical reactions that only require light of 365 nm in wavelength. Since the anodic bonding between silicon substrates and glass substrates has been well established,[9] Pyrex wafers could be used, especially in the cases of high temperature applications. The need to incorporate a substrate for deeper UV detection and reaction, however, requires the use of quartz wafers in place of Pyrex wafers. Bonding quartz and silicon wafers poses a difficult fabrication problem. Anodic bonding between silicon and Pyrex wafers relies on the presence of sodium ions, which are not present in quartz. Furthermore, direct fusion bonding cannot be used because it is a high temperature process: the thermal mismatch of quartz and silicon creating large stress at the interface after annealing is problematic. Jackman *et al.*[7] have demonstrated bonding quartz wafer to quartz wafer with a photodefinable epoxy (SU-8). The detection devices fabricated with that method were compatible with our model reaction. For a wider chemical compatibility, however, we used a cyclic perfluoro polymer (CPFP), CYTOP™, developed as a low dielectric-constant material by Asahi Glass Co., Ltd. (Japan). It is chemically similar to polytetrafluoro ethylene (PTFE), and therefore chemically inert.[10] CYTOP™ can be easily spin-coated or dip-coated on substrates, and used as a bonding material.[11] This process is a relatively low temperature process. The bonding temperature, 160 °C, does not create significant thermal mismatch between quartz and silicon substrates. In fact, CYTOP™ is better than SU-8 for this application because (i) it is chemically more robust (being able to withstand most chemicals found in the clean room except perfluorinated solvents[10, 11]); (ii) it is UV-transparent and therefore does not need to be patterned; (iii) it eliminates the lithography step that SU-8 requires to crosslink it. In our devices, CYTOP™ provided the fluidic seal, and was inert to chemicals used in all experiments.

3.2. Model chemistry

To test designs of the microfabricated reactors, the pinacol formation reaction of benzophenone in isopropanol was used as a model reaction (reaction (1)).

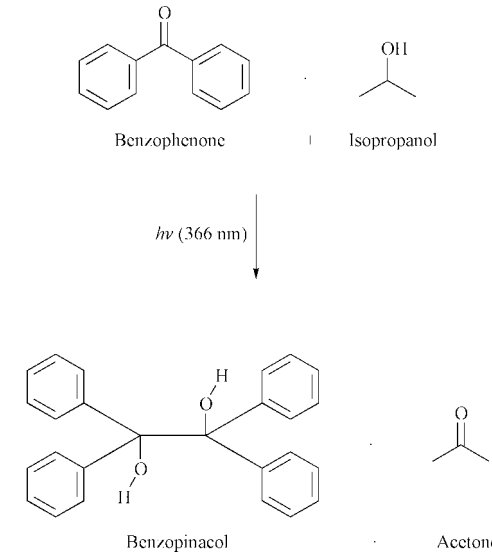

(1)

This reaction is known to follow a radical reaction pathway (reactions (2)–(4)), in which benzopinacol, benzophenone, and the mixed-pinacol along with many radical species are generated.[12]

$$Ph_2CO + h\nu \rightarrow Ph_2CO^* \rightarrow Ph_2CO^{**} \quad (2)$$

$$Ph_2CO^{**} + (CH_3)_2CHOH \rightarrow Ph_2COH^{\cdot} + (CH_3)_2C^{\cdot}OH \quad (3)$$

$$Ph_2CO + HO(CH_3)_2C^{\cdot} \rightarrow Ph_2COH^{\cdot} + (CH_3)_2CO \quad (4)$$

Once the high-energy excited state of benzophenone is formed, the subsequent reactions proceed without additional photons. It has also been observed that a highly absorbent intermediate is formed in the reaction, but is short-lived and oxygen-sensitive.[13] Reactions (3) and (4) occur after the irradiation consuming an additional benzophenone molecule, and it takes a long period of time (more than 24 h) for the completion of these reactions.[12] We found that on-line UV spectroscopic analysis was indicative of the course of reaction, and could be verified with off-line analysis when the reactions were complete.

In the UV detection scheme, since 0.5 M benzophenone solution is a concentrated solution, Beer's law does not apply, and the commonly reported molar absorption coefficient cannot be used. The absorption was estimated experimentally before reactor design. The detector microchip has a path length of 0.05 mm, which passes 60% of light to the detector (measured experimentally); on the other hand, the reactor chip has a depth of ~0.25 mm, allowing the absorption of most of the incident light. If a 0.5 M solution was used in macro-scale reaction systems, it would be an optically thick solution where most of the light is absorbed in the first few hundreds of microns next to the light source, and the rest of the solution does not participate in the reaction. We have thus attained a more efficient absorption scheme in the microreactors by reducing the physical thickness of the reaction fluid.

Fig. 4 shows UV absorption of reaction mixture at different flow rates superimposed on UV responses of standard solutions of the reactant benzophenone. These curves follow identical shapes to the ones obtained with conventional UV-spectroscopic equipment found in the literature.[12] The UV absorbance of the final pinacol product is small compared to that of the starting material, benzophenone, and therefore the absorbance of the benzopinacol is assumed not to contribute.[12,13] The radical intermediates also absorb UV light at specific wavelengths between 300 and 400 nm. We believe that these radicals contribute to the slight shift of the maximum of the absorbance curves compared to the standard curves (Fig. 4). Nonetheless, because the concentration of these intermediate species is small compared to the starting material and the product, the absorbance measurements provide a measure of the extent of reactions on chip, and the results agree well with the HPLC analysis of the final product mixture.

The absorbance of reaction mixture as shown in Fig. 4 can be correlated to the on-chip conversion of benzophenone. We measured the rate of disappearance of benzophenone by comparing absobance measurements of the reaction mixture to those of the standard solutions. The results from setup I in Fig. 5(A) demonstrate that the on-chip conversion of benzophenone due to UV irradiation is a function of the flow rate, or equivalently, the residence time on chip. It should be noted, however, that there is a finite volume between the two mounts, and therefore the delay in the detection varies inversely with the flow rate. We believe the conversion of benzophenone due to irradiation still dominates over the residence time effect.

For the overall reaction, the longer the residence time, the greater the conversion of the reactant as expected. We observe that there is almost no measurable on-chip conversion of the reactant for flow rates that are above 10 μl min^{-1}. A plausible explanation for this observation follows from the analysis of various time scales. Because the residence time is so small, the amount of absorbed light by the reactant only creates a small concentration of high-energy species near the light source. These species do not have long enough residence time to diffuse very far into the solution or to react, *i.e.* the time scale for flow (residence time) is smaller than both the diffusion time scale and the reaction time scale. With reduced flow rates (large residence times), the conversion improves because the amount of light absorbed increases, and there is sufficient time for the excited species to diffuse and react with benzophenone.

The conversion estimated from the on-line spectroscopic measurement was confirmed by the off-line analysis (after at least 48 h). Fig. 5(B) shows the conversion as a function of flow rate determined by HPLC separation (with UV detection). The trend agrees with that obtained from on-line UV absorbance measurement, indicating that the conversion is a function of the feed flow rate. The conversion measured in the HPLC analysis is larger since the analysis was performed after the dark reactions were complete. Nevertheless, it is evident that the on-line UV absorbance measurement is a practical indicator of the extent of reaction, and therefore can be used to monitor the progress of the reaction *in situ*. The difference between initial conversion and that after dark reactions suggests that the photochemical microreactors could be used for photoinitiation of reactions to be completed in storage vessels.

In these experiments, using microreactors also proved to be practical in terms of cleaning and reusing these devices. Benzopinacol has a low solubility in isopropanol, so in bench scale reactions, benzopinacol separates out from the reaction mixture, forming white crystals in the reaction flask.[8] In all but one of the experiments in this work, no crystals formed while on the microreactor chip†because the concentration of benzopinacol on chip did not exceed the saturation concentration. When the samples were collected, however, crystals precipitated out of the solution gradually in the storage vials due to dark reactions. The microreactor implementation is advantageous for reactions that only need initiation with UV light and propagate with radicals. Shrinking the length scale not only avoids undesirable crystallization (therefore eliminating the need for cleaning), but also changes the characteristic time of transport relative to reaction kinetics and improves the efficiency.

The overall quantum efficiency (η) of the reaction on-chip was defined by

$$\eta = \frac{\text{moles of reaction (disappearance of reactant)}}{\text{moles of photons}}$$

In this set of experiments, η was estimated by the ratio of the conversion of benzophenone measured from HPLC analysis and the amount of light that was emitted from the miniature UV lamp. In calculating the amount of the light from the mini UV

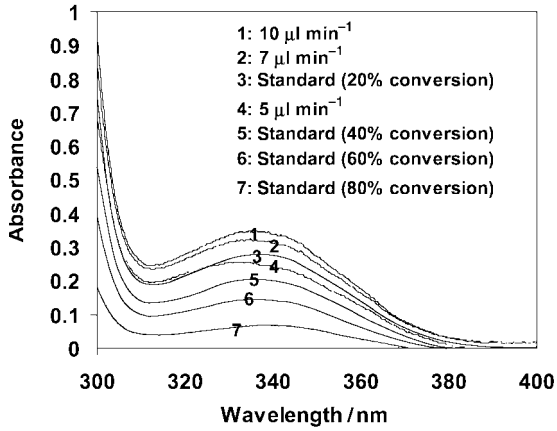

Fig. 4 UV absorption of reaction mixture at different flow rates, thus different residence time. The solid curves are absorption spectra of reaction mixtures run at different flow rates (from top to bottom: 10 μl min^{-1}, 7 μl min^{-1}, and 5 μl min^{-1}). The faint curves are the standard curves (from top to bottom: 20% conversion, 40% conversion, 60% conversion, and 80% conversion of benzophenone).

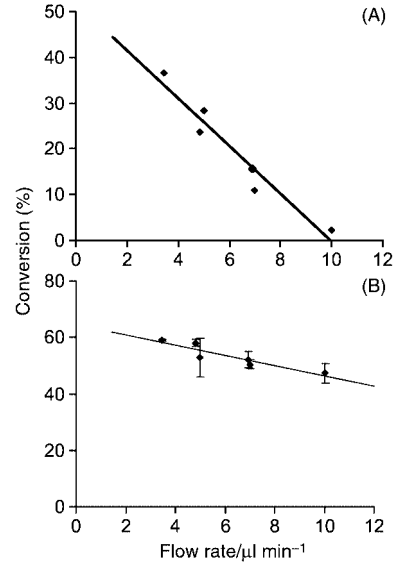

Fig. 5 (A) Conversion of benzophenone estimated from on-line UV spectral data as a function of flow rate of the starting material, showing the relationship between residence time and conversion. (B) HPLC data demonstrating the relationship between flow rate and conversion of benzophenone.

† We have observed that for very low flow rates (< 3 μl min^{-1}), crystals would form on the chip, clog the channel and stop the flow over time.

lamp, we measured the power from the lamp and scaled it assuming a uniform power density due to the slightly larger chip-area compared to the detector area. The light output was filtered to give light of 365 nm in wavelength. The number of moles of photons was then calculated from the power of the lamp assuming 365 nm as the average wavelength.

The computed quantum yields are shown in Fig. 6 as a function of flow rate. The quantum yields agree in the order of magnitude with those determined for conventional photochemical reaction setups.[12] At higher flow rates, the quantum efficiency is larger than the reported value for conventional systems. The trend of the overall quantum efficiency suggests that the light is used less efficiently at lower flow rates. This observation may be explained in terms of the decrease in the optical density of the solution with conversion of benzophenone. As benzophenone is converted in the reaction process, more light passes through the liquid, and is not used in the reaction.

In order to eliminate the delay for detection in setup I, we have implemented a monolithic integrated device. setup II detects the reaction mixture with only a few seconds of delay on chip (see Fig. 2(A) for overall chip design). We observed no interference from the miniature UV lamp for reaction on the UV spectra (data not shown).The reactions were again monitored by on-line UV spectrometry. In these experiments, the UV spectra of the reactive solutions exhibited higher absorbance than unreacted solutions as shown in Fig. 7, indicating the formation of the highly absorbant intermediate. We believe that there are two factors contributing to the different absorption spectra in the analogous experiments with the two-chip setup. First, reactions proceeded in the tubing between the reaction chip and the detection chip and their mounts, reducing the amount of the intermediate. Secondly, small amounts of oxygen may have permeated into the system between the reaction chip and the detection chip, reacting with the oxygen-sensitive intermediate. In general, for other reactions where no interfering intermediates are formed, the monolithic integration scheme would be more desirable since it eliminates the delay before detection. In this case, however, the presence of a strongly absorbing short-lived intermediate interferes with conversion measurements in the monolithically integrated device.

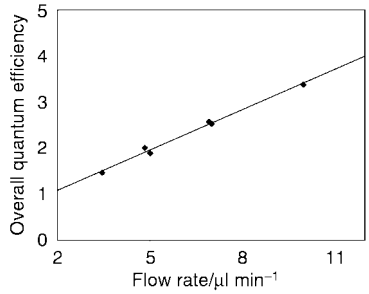

Fig. 6 Quantum efficiency estimation: these calculations are based on measured output rate of light source, and conversion of reactant based on HPLC measurements.

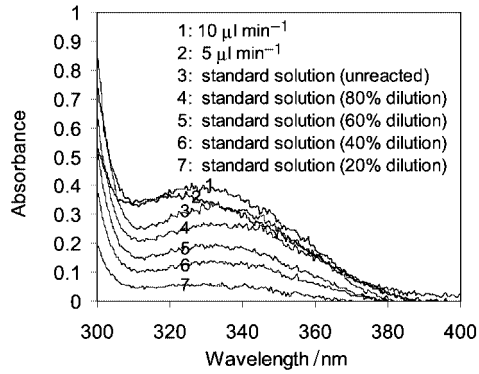

Fig. 7 Reaction and on-line detection of the monolithically integrated device. The curves demonstrate the shift in absorbance peak, indicating the presence of the intermediate species; two different flow rates also yield different responses in UV absorbance indicating reaction progress (top most solid curve for 10 μl min^{-1}, and the one below for 5 μl min^{-1}).

4. Conclusions

In the present work, we have demonstrated the practicality of photochemical reactions (exemplified with photo-pinacolation of benzophenone in isopropanol) with a miniaturized light source on microfabricated chips. The advantages of the small-scale reactors are that the efficiency of photon transfer and reactions can be increased. In particular, with optically thick solutions, microreactors offer the opportunity of "thinning" the solutions to make the most use of the incident light. Crystallization can be avoided in the reactor with a continuous flow system by controlling residence time, and consequently the extent of reaction on-chip, making downstream processes simpler. The two-chip integration is simpler in design, and the delay allowed the short-lived intermediate to react so that the benzopinacol formation reaction could be monitored using UV spectroscopy. The monolithically integrated device, however, provided a true on-line immediate analysis of the reaction mixture. Parallel operations of multiple miniaturized reaction devices presented in this work may enable process intensification, and the on-line detection provides an opportunity for fast process optimization. The potential applications of this technology are likely in organic synthesis and photo-initiated polymerization reactions of small scale. Running deprotection reactions on chip might increase the efficiency and accelerate the processes. In the case of photopolymerization reactions, the microchips can be used for the initiation reactions and the polymerization reactions could be finished in storage vessels designated for polymerization. In fabricating these microreaction devices, we have demonstrated a low temperature bonding of quartz substrates to micro-machined silicon devices with a perfluorinated polymer—CYTOP™. Because of its inertness and process simplicity, CYTOP™ may prove to be useful in many other microreactor applications.

Acknowledgements

The research was supported by DARPA under the Microflumes Project, and National Science Foundation graduate fellowship program to HL. The technical assistance from the staff of the Microsystems Technology Laboratories, and Prof. T. F. Jamison and S. Patel in the Department of Chemistry at MIT are gratefully acknowledged. We also thank Dr R. J. Jackman for inspiration and helpful discussions, and C. D. Albritton for help with experiments.

References

1 R. Roberts, R. P. Ouellette, M. M. Muradaz, R. F. Cozzens and P. N. Cheremisinoff, *Applications of Photochemistry*, Technomic Publishing Co., Inc., Lancaster, Pennsylvania, 1984.
2 H Bottcher, J. Bendig, M. A. Fox, G. Hopt and H. Timpe, *Technical Applications of Photochemistry*, Deutscher Verlag fur Grundstoffindustrie, Leipzig, 1991.
3 T. W. Greene, *Protective Groups in Organic Synthesis*, Wiley, New York, 2nd ed., 1991.

4 K. F. Jensen, *Chem. Eng. Sci.*, 2001, **56**, 293.★ *Significant reference*.
5 A. A. Ayon, R. Braff, C. C. Lin, H. H. Sawin and M. A. Schmidt, *J. Electrochem. Soc.*, 1999, **146**, 339.★ *Significant reference*.
6 M. W. Losey, M. A. Schmidt and K. F. Jensen, *Ind. Eng. Chem. Res.*, 2001, **40**, 2555.
7 R. J. Jackman, T. M. Floyd, R. Ghodssi, M. A. Schmidt and K. F. Jensen, *J. Micromech. Microeng.*, 2001, **11**, 263.★ *Significant reference*.
8 B. S. Furniss, A. J. Hannaford, P. W. G. Smith and A. R. Tatchell, *Vogel's Textbook of Practical Organic Chemistry*, Addison Wesley Longman Ltd., Longman Group UK Ltd., 1989.
9 M. A. Schmidt, *Proc. IEEE*, 1988, **86**, 1575.
10 L. Asahi Glass Co., *CYTOP Tech. Rep.*, 1111, 1.
11 A. Han, K. W. Oh, S. Bhansali, H. T. Henderson and C. H. Ahn, *A Low Temperature Biochemically Compatible Bonding Technique Using Fluoropolymers for Biochemical Microfluidic Systems in Proceedings of IEEE MEMS Conference*, Miyazaki, Japan.★ *Significant reference*.
12 J. N. Pitts, R. L. Letsinger, R. P. Taylor, J. M. Patterson, G. Recktenwald and R. B. Martin, *J. Am. Chem. Soc.*, 1959, **81**, 1068.★ *Significant reference*.
13 J. Chilton, L. Giering and C. Steel, *J. Am. Chem. Soc.*, 1976, **98**, 1865.